J. Mech. Phys. Solids Vol. 40, No. 4, pp. 739–765, 1992.
Printed in Great Britain.

0022-5096/92 $5.00 + 0.00

FRACTURE MECHANICS FOR PIEZOELECTRIC CERAMICS

Z. SUO

Department of Mechanical Engineering, University of California, Santa Barbara, CA 93106-5070, U.S.A.

C.-M. KUO

Division of Applied Mechanics, Stanford University, Stanford, CA 94305-4040, U.S.A.

D. M. BARNETT

Department of Materials Science and Engineering, Stanford University, Stanford, CA 94305-2205, U.S.A.

and

J. R. WILLIS

School of Mathematical Sciences, University of Bath, Bath BA2 7AY, U.K.

(*Received* 15 *March* 1991; *in revised form* 30 *June* 1991)

ABSTRACT

WE STUDY cracks either in piezoelectrics, or on interfaces between piezoelectrics and other materials such as metal electrodes or polymer matrices. The projected applications include ferroelectric actuators operating statically or cyclically, over the major portion of the samples, in the linear regime of the constitutive curve, but the elevated field around defects causes the materials to undergo hysteresis locally. The fracture mechanics viewpoint is adopted—that is, except for a region localized at the crack tip, the materials are taken to be linearly piezoelectric. The problem thus breaks into two subproblems: (i) determining the macroscopic field regarding the crack tip as a physically structureless point, and (ii) considering the hysteresis and other irreversible processes near the crack tip at a relevant microscopic level. The first subproblem, which prompts a phenomenological fracture theory, receives a thorough investigation in this paper. Griffith's energy accounting is extended to include energy change due to both deformation and polarization. Four modes of square root singularities are identified at the tip of a crack in a homogeneous piezoelectric. A new type of singularity is discovered around interface crack tips. Specifically, the singularities in general form two pairs: $r^{1/2+i\varepsilon}$ and $r^{1/2+i\kappa}$, where ε and κ are real numbers depending on the constitutive constants. Also solved is a class of boundary value problems involving many cracks on the interface between half-spaces. Fracture mechanics are established for ferroelectric ceramics under small-scale hysteresis conditions, which facilitates the experimental study of fracture resistance and fatigue crack growth under combined mechanical and electrical loading. Both poled and unpoled ferroelectric ceramics are discussed.

1. INTRODUCTION

1.1. *Piezoelectricity and ferroelectric ceramics*

PIEZOELECTRICS deform when subjected to an electric field and polarize when stressed. The stress σ, strain γ, electric induction D, and electric field E obey the constitutive relations

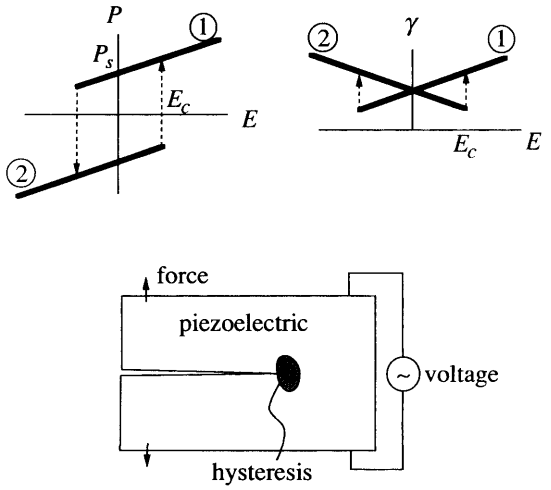

FIG. 1. Idealized ferroelectric hysteresis consists of two piezoelectric branches. P_S is the spontaneous polarization and E_C the coercive field. A crack intensifies stress and induction, causing local hysteresis and possibly fatigue. The sample is piezoelectric outside the small hysteresis zone at the crack tip.

$$\sigma = C\gamma - eE, \quad D = \varepsilon E + e\gamma, \tag{1.1}$$

where C is the elasticity, ε the permittivity and e the piezoelectricity; these tensors are material-specific. For example, quartz is piezoelectric, with the physical constants on the orders

$$C \sim 10^{11}\ \mathrm{N/m^2}, \quad \varepsilon \sim 10^{-11}\ \mathrm{F/m}, \quad e \sim 10^{-1}\ \mathrm{C/m^2}. \tag{1.2}$$

Ferroelectrics belong to a subgroup which, when in the form of a single domain, possess a spontaneous polarization that can be reversed by applying a high electric field, the coercive field. Most ferroelectrics are also linearly piezoelectric when operating around the spontaneous polarization. Figure 1 illustrates the idealized ferroelectric behaviors, switching between two piezoelectric branches. Since the 1940s, these properties have been exploited to produce polycrystalline piezoelectrics: macroscopic polarization is induced in ceramics by applying a high static field, which partially aligns the polar axes in the randomly oriented domains, a process called poling. The physical constants for poled barium-titanate ($BaTiO_3$) and lead-zirconate-titanate are on the orders

$$C \sim 10^{11}\ \mathrm{N/m^2}, \quad \varepsilon \sim 10^{-8}\ \mathrm{F/m}, \quad e \sim 10\ \mathrm{C/m^2}. \tag{1.3}$$

Both ε and e for the ceramics are substantially higher than for quartz. Unpoled ferroelectric ceramics do not have macroscopic piezoelectricity but still have large permittivity, so they make good capacitors.

A dimensionless group is formed by the three types of moduli, varying for most materials in the range

$$e/\sqrt{\varepsilon C} = 0.1\text{–}1. \tag{1.4}$$

This number indicates the degree of the electromechanical coupling.

Books that contain the background information include FATUZZO and MERZ (1967) on domain walls, JAFFE *et al.* (1971) on ceramics processing, POHANKA and SMITH (1987) on fracture testing and polymer matrix composites, and MIKHAILOV and PARTON (1990) on electroelasticity.

1.2. *Cracking and fatigue*

Ferroelectric ceramics are brittle (toughness ≈ 1 MPa $m^{1/2}$) and susceptible to cracking at all scales from domains to devices. When a ceramic is poled by a static field on the order of MV/m, cracks nucleate to relax the incompatible strains (CHUNG *et al.*, 1989). Ferroelectric thin films can sustain high fields without electric breakdown, but may delaminate from the substrate, or crack laterally. Actuators are usually layered with substrates, or embedded in polymer matrices. Interface debonding degrades the electrical performance. Many static and cyclic failure behaviors in multilayer actuators are described by WINZER *et al.* (1989).

There has recently been a resurgence in the effort to develop non-volatile memory devices based on ferroelectric hysteresis. The major material challenge has been fatigue: the hysteresis loops diminish with the cycling. Many fatigue mechanisms have been postulated. Microcracking is one mechanism responsible for fatigue, which grows with cycling, forming micro-capacitors. Another mechanism involves *a*-domains that grow from the surface and hinder the motion of 180° domain walls (HAYASHI *et al.*, 1964). The stress state plays an important role in these mechanisms, as shown by HE *et al.* (1991). PAN *et al.* (1989) found that the number of cycles to failure can be greatly increased by carefully polishing the ceramic surfaces prior to electroding.

Ferroelectric hysteresis degrades materials even if samples operate nominally in the linear piezoelectric regime. Under an alternating low amplitude field, the field concentrated around defects can cause materials to undergo hysteresis locally. Fatigue crack growth is likely, although no systematic study has been made. We will develop a mechanics framework to evaluate fatigue crack growth under small-scale hysteresis (see Fig. 1). The terminology will be borrowed from fatigue crack growth in metals under small-scale yielding conditions, although the underlying physics may be entirely different for the two phenomena.

Fracture testing has been conducted for ferroelectric ceramics (POHANKA and SMITH, 1987; FREIMAN and POHANKA, 1989). Ordinary fracture mechanics ignoring piezoelectricity has been used to interpret data. One theme of this paper is to introduce the electric intensity factor K_{IV}, analogously to the stress intensity factor in the usual fracture mechanics, as a correlating parameter, so that failure testing can be interpreted in the full range of mechanical and electrical loadings. A second theme is to analyze interface cracks for applications in multilayer actuators.

1.3. *Boundary conditions*

Cracks in piezoelectrics have been investigated as an electroelastic problem by several authors. Contributions of the Soviet scientists have been reviewed by MIKHAILOV and

Parton (1990). Parton (1976) took a crack to be a traction-free, but permeable, slit—that is, the potential and the normal component of the induction are continuous across the slit:

$$\phi^+ = \phi^-, \quad D_n^+ = D_n^-. \tag{1.5}$$

These boundary conditions cannot be defended on physical grounds. Specifically, for piezoelectric ceramics, the permittivity is 10^3 times higher than the environment (e.g. air or silicone oil). A crack may be thought of as a low-capacitance medium carrying a potential drop.

Deeg (1980) and Pak (1990) proposed another set of boundary conditions on the crack:

$$D_n^+ = D_n^- = 0. \tag{1.6}$$

Two assumptions are involved, namely: (i) no external charge resides on either crack face, and (ii) the electric induction in the environment is negligible. On the basis of these boundary conditions, Pak (1990) studied a crack with its front coincident with the poling axis, and Sosa and Pak (1990) investigated the more general crack tip field using an eigenfunction analysis. Shindo *et al.* (1990) analyzed cracks in piezoelectric layers using integral equation methods. Kuo and Barnett (1991) carried out an asymptotic crack tip analysis, and found various singularities depending on the crack face boundary conditions, for an interface crack between bonded piezoelectrics. The allowable singularities differ in one respect from those associated with the elastic interface cracks, which we shall illustrate in the present work.

In his calculation of the electrostrictive stress near a crack tip, McMeeking (1989) pointed out that (1.6) may not be appropriate for small crack opening. He modeled the crack as an elliptic flaw with lower permittivity. The parameter

$$(\varepsilon_f/\varepsilon_m)(a/b) \tag{1.7}$$

emerges, where ε_f and ε_m are the permittivities of the flaw and the matrix, respectively, and a and b are the semi-axes of the ellipse ($a > b$). Assumption (1.6) corresponds to the case that parameter (1.7) is small. However, it may not be small even if the permittivity ratio is small, because a/b can be huge for crack-like flaws. Similar behavior emerges for piezoelectrics, which will not be discussed here.

McMeeking (1987, 1990) also modeled cracks in dielectrics containing a conducting fluid. The appropriate boundary condition is then

$$\phi^+ = \phi \quad = 0. \tag{1.8}$$

An analysis of conducting cracks in piezoelectrics has been carried out by Suo (1992).

We shall adopt (1.6) in this article, since most results are directed towards establishing a framework for macroscopic fracture testing of ferroelectric ceramics, where the crack separation is large except for a small zone near the crack tip. From the viewpoint of the fracture mechanics, this zone can be treated as a small-scale feature, lumped into the macroscopically measured toughness.

1.4. *Plan of this paper*

In Section 2, the elements of elasticity, electrostatics and thermodynamics are combined for ease of reference. In Section 3, Griffith's energy accounting is extended to include the electrical energy. Examples are given for which exact energy release rates are readily obtained. It is found that an electrical loading usually provides a negative energy release rate. Whether this negative driving force will retard crack growth will depend on the fracture mechanism at the crack tip.

To investigate the crack tip stress field, in Section 4 a general solution to the electroelastic problem is obtained, involving four analytic functions of different variables. The electroelastic field around a crack tip in a homogeneous piezoelectric is given in Section 5. It contains four modes of square root singularities, but only one mode (mode I) gives rise to the tension directly ahead of the crack. A class of boundary value problems is solved, including that of a crack in an infinite piezoelectric.

The analysis is then extended to cracks on interfaces between different materials in Section 6. A new type of singularity, first reported by KUO and BARNETT (1991), emerges from this analysis. Specifically, the four singularities form two pairs: $r^{-1/2\pm i\varepsilon}$ and $r^{-1/2\pm\kappa}$. The latter pair is peculiar, seemingly violating the singularity orders suggested by the J-integral. We demonstrate that these singularities are indeed consistent with path-independence of the J-integral. The solution for a finite crack on an interface is also given.

We study the mechanics implications of our results in Section 7. Both unpoled and poled ferroelectric ceramics are treated. A pragmatic approach is described to evaluate fracture resistance, and fatigue crack growth of ferroelectrics.

2. Basic Equations of the Continuum Theory

Subject a material to a field of displacement $\mathbf{u}$ and electric potential ϕ. The strain γ and the electric field $\mathbf{E}$ are derived from gradients:

$$\gamma_{ij} = \tfrac{1}{2}(u_{i,j}+u_{j,i}), \quad E_i = -\phi_{,i}. \tag{2.1}$$

Attention is limited to small deformation in this work.

The stress σ and the electric induction $\mathbf{D}$ are defined such that, across an interface, they jump by

$$n_i[\sigma_{ij}^{+}-\sigma_{ij}^{-}] = t_j, \quad n_i[D_i^{+}-D_i^{-}] = -\omega, \tag{2.2}$$

where $\mathbf{n}$ is the unit normal to the interface pointing from the $+$ side; $\mathbf{t}$ is the force and ω the charge, per unit area, externally supplied on the interface. σ and $\mathbf{D}$ are divergence-free, i.e.

$$\sigma_{ij,i} = 0, \quad D_{i,i} = 0. \tag{2.3}$$

Here the body force and extrinsic bulk charge are taken to be negligible.

The principle of virtual work is

$$\int \sigma_{ij}\gamma_{ji}\,\mathrm{d}v = \int n_i\sigma_{ij}u_j\,\mathrm{d}s, \quad \int D_iE_i\,\mathrm{d}v = -\int n_iD_i\phi\,\mathrm{d}s, \tag{2.4}$$

where v is the volume and s the surface of the body. Any two among (2.1), (2.3) and (2.4) imply the third.

Analogies may be drawn between the mechanical and electrical variables according to their roles in the above equations, such as $\gamma \sim E, u \sim \phi, \sigma \sim D$ and $t \sim \omega$. However, it is γ and $\mathbf{D}$ together that define the physical distortion of the material. They are assumed to be reversible, so that an energy function, $\psi(\gamma, \mathbf{D})$, exists, for which

$$\mathrm{d}\psi = \sigma_{ij}\,\mathrm{d}\gamma_{ji} + E_i\,\mathrm{d}D_i. \tag{2.5}$$

We will focus on materials in the stable regime, where ψ is convex in the $(\gamma, \mathbf{D}, \psi)$-space. This class of nonliner materials is general enough to include the poled ferroelectrics operating around the remanent state, and electrostrictive ceramics.

We shall formulate the theory based on $\mathbf{u}$ and ϕ. A more convenient energy function $w(\gamma, \mathbf{E})$, the electric enthalpy, is defined by

$$w = \psi - E_iD_i. \tag{2.6}$$

Evidently, w is not convex in the $(\gamma, \mathbf{E}, w)$-space: it has a saddle point at $(\mathbf{E}, \gamma) = (0, 0)$. A Legendre transformation shows that

$$\mathrm{d}w = \sigma_{ij}\,\mathrm{d}\gamma_{ji} - D_i\,\mathrm{d}E_i. \tag{2.7}$$

The stress and the electric induction are therefore given by

$$\sigma_{ij} = \partial w/\partial\gamma_{ji}, \quad D_i = -\partial w/\partial E_i. \tag{2.8}$$

Ferroelectrics are approximately linear when the loading amplitude is small compared to the depoling field. Linear piezoelectrics are described by a quadratic

$$w = \tfrac{1}{2}C_{ijrs}\gamma_{ji}\gamma_{rs} - \tfrac{1}{2}\varepsilon_{is}E_iE_s - e_{irs}E_i\gamma_{rs}, \tag{2.9}$$

where C is the stiffness, ε the permittivity and e the piezoelectricity. The following reciprocal symmetries hold:

$$C_{ijrs} = C_{srji}, \quad \varepsilon_{is} = \varepsilon_{si}. \tag{2.10}$$

Other symmetries implied by the symmetry of the strain tensor, such as

$$C_{ijrs} = C_{jirs} = C_{ijsr}, \quad e_{irs} = e_{isr}, \tag{2.11}$$

are of less significance, and will not be invoked in the theoretical development. For stable materials, both C and ε are positive definite, i.e.

$$C_{ijrs}\gamma_{ji}\gamma_{rs} > 0, \quad \varepsilon_{is}E_iE_s > 0, \tag{2.12}$$

for any real non-zero real tensor γ and vector $\mathbf{E}$.

Derived from (2.9) and (2.8), the constitutive relations for linear piezoelectrics are

$$\sigma_{ij} = C_{ijrs}\gamma_{rs} - e_{sji}E_s, \quad D_i = \varepsilon_{is}E_s + e_{irs}\gamma_{rs}. \tag{2.13}$$

This is the tensor form of (1.1). An alternative expression using σ and $\mathbf{E}$ as controlling quantities is

$$\gamma_{ij} = S_{ijrs}\sigma_{rs} + d_{sji}E_s, \quad D_i = \varepsilon^{\sigma}_{is}E_s + d_{irs}\sigma_{rs}, \tag{2.14}$$

where S is the compliance, d is the piezoelectric strain tensor and ε^{σ} is the stress-free permittivity [which is different from ε in (2.13)]. The moduli in (2.13) and (2.14) are obviously related.

Given a ceramic sample, the mechanical boundary conditions are taken to be

$$n_i\sigma_{ij} = t^0_j, \quad \text{on } s_t, \tag{2.15a}$$

$$u_j = u^0_j, \quad \text{on } s_u, \tag{2.15b}$$

where the superscript 0 indicates the prescribed values. The electric boundary conditions are

$$n_iD_i = -\omega^0, \quad \text{on } s_\omega, \tag{2.16a}$$

$$\phi = \phi^0, \quad \text{on } s_\phi. \tag{2.16b}$$

In the above, the stress and induction in the environment are assumed to be negligible. The normal $\mathbf{n}$ directs towards the environment.

Define a functional

$$\Omega(\mathbf{u}, \phi) = \int_v [\tfrac{1}{2}C_{ijrs}u_{j,i}u_{r,s} - \tfrac{1}{2}\varepsilon_{is}\phi_{,i}\phi_{,s} + e_{irs}\phi_{,i}u_{r,s}]\,\mathrm{d}v - \int_{s_t} t^0_j u_j\,\mathrm{d}s + \int_{s_\omega} \omega^0\phi\,\mathrm{d}s. \tag{2.17}$$

Of all the fields $(\mathbf{u}, \phi)$ satisfying (2.15b) and (2.16b), the solution field renders

$$\delta\Omega = 0. \tag{2.18}$$

A finite element procedure can be formulated using this variational principle, with four degrees of freedom, u_1, u_2, u_3 and ϕ, at each node. Since w is not positive definite, the solution field need not minimize Ω.

Although the relevant energy function, w, is indefinite, uniqueness can be stated for a fairly general class of nonlinear materials under small deformation. Let $(\sigma, \gamma, u, D, E, \phi)$ and $(\tilde{\sigma}, \tilde{\gamma}, \tilde{u}, \tilde{D}, \tilde{E}, \tilde{\phi})$ be different solutions satisfying the same boundary conditions (2.15) and (2.16), so that the difference field does not do any virtual work on the surface:

$$\int_s \{n_i(\sigma_{ij} - \tilde{\sigma}_{ij})(u_j - \tilde{u}_j) - n_i(D_i - \tilde{D}_i)(\phi - \tilde{\phi})\}\,\mathrm{d}s = 0. \tag{2.19}$$

Next consider the internal virtual work

$$\int_v \{(\sigma_{ij} - \tilde{\sigma}_{ij})(\gamma_{ji} - \tilde{\gamma}_{ji}) + (D_i - \tilde{D}_i)(E_i - \tilde{E}_i)\}\,\mathrm{d}v. \tag{2.20}$$

It must also vanish as implied by the principle of virtual work (2.4). However, the integrand is positive for stable materials. The contradiction proves uniqueness. As an example, for the linear material defined by (2.13), the integrand in (2.20) can be written as

$$C_{ijrs}(\gamma_{ji}-\tilde{\gamma}_{ji})(\gamma_{rs}-\tilde{\gamma}_{rs})+\varepsilon_{is}(D_i-\tilde{D}_i)(D_s-\tilde{D}_s), \tag{2.21}$$

which is positive because C and ε are positive definite.

3. Energy Considerations

Griffith's energy accounting is applicable to the non-linear reversible materials defined by (2.5). Let two such materials be bonded, with a crack area A left on the interface, the crack faces being free of external charge and traction. Load the system by a generalized displacement Δ and voltage V, with F and Q the associated force and charge. The electric enthalpy W in the body, which is the volume integral of w, accumulates according to

$$\mathrm{d}W = F\,\mathrm{d}\Delta - Q\,\mathrm{d}V - \mathscr{G}\,\mathrm{d}A. \tag{3.1}$$

This equation defines $\mathscr{G}$ as the driving force for the crack area A, as well as demonstrating that F and Q drive Δ and V. When the crack area is fixed, $\mathrm{d}A = 0$, so that (3.1) recovers (2.4), with the identifications

$$F\Delta = \int n_i\sigma_{ij}u_j\,\mathrm{d}s, \quad QV = -\int n_iD_i\phi\,\mathrm{d}s. \tag{3.2}$$

Equivalent definitions of $\mathscr{G}$ can be derived using Legendre transformations. For example, using the potential energy $\Pi = W - F\Delta$ gives

$$\mathrm{d}\Pi = -\Delta\,\mathrm{d}F - Q\,\mathrm{d}V - \mathscr{G}\,\mathrm{d}A. \tag{3.3}$$

The functions W and Π can be viewed as the total energy of the system, comprising the body and its loading device, with the relevant function in any given problem depending on the type of boundary conditions applied.

Consistent with the above, $\mathscr{G}$ can be rewritten as

$$\mathscr{G} = -(\partial W/\partial A)_{\Delta,V} = -(\partial\Pi/\partial A)_{F,V}. \tag{3.4}$$

For example, if Δ is maintained by grips and V by electrodes, $\mathscr{G}$ is the *decrease* in energy W associated with the creation of a unit crack area.

For a bimaterial with the interface along the x-axis, the integral

$$J = \int (wn_1 - n_i\sigma_{ip}u_{p,1} - n_iD_i\phi_{,1})\,\mathrm{d}s \tag{3.5}$$

vanishes over contours not enclosing any singularity. When the crack faces are free of external charge and traction

$$\mathscr{G} = J, \tag{3.6}$$

where the J-integral is taken over any path that begins at one point on the lower crack face and ends at another point on the upper crack face. These are extensions of the elastic version due to Rice (1968).

In general, for a given specimen $\mathscr{G}$ can be computed by analyzing the piezoelectric

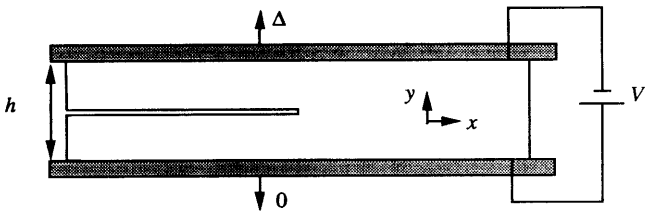

FIG. 2. Piezoelectric slab loaded by separation and voltage.

problem, but rudimentary mechanics will suffice for the following examples. Figure 2 illustrates a cracked piezoelectric slab, of thickness h, electroded and gripped on the top and bottom surfaces. The wake far behind the crack tip is free from the strain and electric field. Far ahead of the crack tip, the non-zero components of strain and electric field are

$$\gamma_{yy} = \Delta/h, \quad E_y = V/h. \tag{3.7}$$

Since Δ and V are held fixed, $\mathcal{G}$ is the decrease in W for a unit advance of the crack, which in turn equals the energy in the volume $h \times 1 \times 1$ of the slab far ahead the tip, and

$$\mathcal{G} = wh = \frac{1}{2h}(C_{yyyy}\Delta^2 - \varepsilon_{yy}V^2 - 2e_{yyy}V\Delta). \tag{3.8}$$

Figure 3 illustrates a double-cantilever-beam subject to applied moments and voltage. The top and bottom surfaces are electroded but traction-free. Since both load and voltage are fixed, $\mathcal{G}$ equals the decrease in energy Π for a unit crack advance:

$$\mathcal{G} = 96S_{xxxx}M^2/h^3 - \tfrac{1}{2}\varepsilon^{\sigma}_{yy}V^2/h. \tag{3.9}$$

Here plane stress conditions are assumed, but plane strain can be treated by a suitable change of moduli. This experiment can be used to determine the effects of the electric field on the toughness of ferroelectric ceramics. The moment may be applied by inserting a wedge and the voltage can be either static or cyclic. Both examples can be treated using the J-integral as done for the elastic versions by RICE (1968).

Observe that for normal operations the contribution to $\mathcal{G}$ from the voltage is small and negative. This negative driving force is entirely physical; for example, it manifests itself in a classical physics experiment, where a dielectric slab partially inserted in a

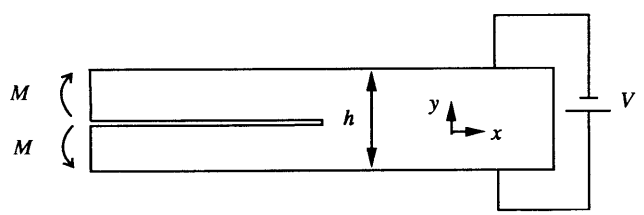

FIG. 3. Double-cantilever-beam loaded by moments and voltage.

parallel-plate capacitor is driven in by this force [see FEYNMAN *et al.* (1964)]. However, whether this force will retard crack growth should depend on the fracture mechanisms at the crack tip. We will discuss this point further in Section 7.

4. COMPLEX VARIABLE SOLUTION

Following a procedure of ESHELBY *et al.* (1953) for anisotropic elasticity, we derive the general solution to the electroelastic problem, which involves four complex variables. For linear piezoelectrics, (2.1) and (2.13) give

$$\sigma_{ij} = C_{ijrs}u_{r,s} + e_{sji}\phi_{,s}, \quad D_i = -\varepsilon_{is}\phi_{,s} + e_{irs}u_{r,s}. \tag{4.1}$$

Substituting into (2.3), one obtains four Navier-type equations for $\mathbf{u}$ and ϕ:

$$(C_{ijrs}u_r + e_{sji}\phi)_{,si} = 0, \quad (-\varepsilon_{is}\phi + e_{irs}u_r)_{,si} = 0. \tag{4.2}$$

Attention will be focussed on two-dimensional problems in the (x, y)-plane, i.e. nothing varies with x_3.

The general solution can be obtained by considering an arbitrary function of a linear combination of x and y:

$$\{u_r, \phi\} = \mathbf{a} f(\zeta_1 x + \zeta_2 y). \tag{4.3}$$

It is convenient, here and in the sequel, to take $\{u_r, \phi\}$ to be a *column* with the entities indicated, so that $\mathbf{a}$ is likewise a four-component column. Without loss of generality, one can always take

$$\zeta_1 = 1, \quad \zeta_2 = p. \tag{4.4}$$

The number p and the column $\mathbf{a}$ are determined by substituting (4.3) into (4.2), which gives

$$(C_{\alpha jr\beta}a_r + e_{\alpha j\beta}a_4)\zeta_\alpha\zeta_\beta = 0, \quad (-\varepsilon_{\alpha\beta}a_4 + e_{\alpha r\beta}a_r)\zeta_\alpha\zeta_\beta = 0, \tag{4.5}$$

where α and β take on the values 1 and 2. This is an eigenvalue problem consisting of four equations; a nontrivial $\mathbf{a}$ exists if p is a root of the determinant polynomial. In Appendix A we prove that (4.5) admits no real root, so the eight roots form four conjugate pairs.

Let p_1, p_2, p_3 and p_4 be the roots with positive imaginary part, $\mathbf{a}_\alpha$ the associated columns, and $z_\alpha = x + p_\alpha y$. The most general real solution is obtained from a linear combination of four arbitrary functions:

$$\{u_r, \phi\} = 2\,\mathrm{Re}\sum_{\alpha=1}^{4}\mathbf{a}_\alpha f_\alpha(z_\alpha). \tag{4.6}$$

For a given boundary value problem, the four functions, f_1, f_2, f_3 and f_4, are sought to satisfy the boundary conditions. The stress and induction are given by

$$\{\sigma_{2j}, D_2\} = 2\,\mathrm{Re}\sum_{\alpha=1}^{4}\mathbf{b}_\alpha f'_\alpha(z_\alpha), \quad \{\sigma_{1j}, D_1\} = -2\,\mathrm{Re}\sum_{\alpha=1}^{4}\mathbf{b}_\alpha p_\alpha f'_\alpha(z_\alpha), \tag{4.7}$$

where, for a pair $(p, \mathbf{a})$, the associated $\mathbf{b}$ is

$$b_j = (C_{2jr\beta}a_r + e_{\beta j2}a_4)\zeta_\beta, \quad b_4 = (-\varepsilon_{2\beta}a_4 + e_{2r\beta}a_r)\zeta_\beta. \tag{4.8}$$

This is derived from (4.1) and (4.3). Substituting (4.8) into (4.5) gives an alternative expression:

$$b_j = -p^{-1}(C_{1jr\beta}a_r + e_{\beta j1}a_4)\zeta_\beta, \quad b_4 = -p^{-1}(-\varepsilon_{1\beta}a_4 + e_{1r\beta}a_r)\zeta_\beta. \tag{4.9}$$

Define 4×4 matrices

$$A = [\mathbf{a}_1, \mathbf{a}_2, \mathbf{a}_3, \mathbf{a}_4], \quad B = [\mathbf{b}_1, \mathbf{b}_2, \mathbf{b}_3, \mathbf{b}_4]. \tag{4.10}$$

Each of the $\mathbf{a}$s is determined by the eigenvalue problem up to a complex-valued normalization constant. Assuming that the four eigenvalues are distinct and following a method in STROH (1958), one can show that both A and B are non-singular.

Define

$$Y = iAB^{-1}, \tag{4.11}$$

where $i = \sqrt{-1}$. We list several properties key to the theoretical development, their proofs being given in Appendix A. First, Y is Hermitian, and independent of the normalization for A. Next divide Y into blocks

$$Y = \begin{bmatrix} Y_{11} & Y_{14} \\ Y_{41} & Y_{44} \end{bmatrix}, \tag{4.12}$$

where Y_{11} is the 3×3 upper left-hand block and Y_{44} is the lower right-hand element. They have different dimensions:

$$Y_{11} \sim [\textit{elasticity}]^{-1}, \quad Y_{44} \sim [\textit{permittivity}]^{-1}, \quad Y_{14} = \bar{Y}_{41}^T \sim [\textit{piezoelectricity}]^{-1}. \tag{4.13}$$

For stable materials, LOTHE and BARNETT (1975) showed that

$$Y_{11} \text{ is positive definite, but } Y_{44} < 0. \tag{4.14}$$

Finally consider an in-plane coordinate rotation

$$R \equiv \left[\frac{\partial x_i^*}{\partial x_j}\right] = \begin{bmatrix} \cos\theta & \sin\theta & 0 \\ -\sin\theta & \cos\theta & 0 \\ 0 & 0 & 1 \end{bmatrix}, \tag{4.15}$$

where (*) indicates the new coordinates, and θ is the rotation angle from x to x^*. The four blocks of Y transform like second-rank tensors, vectors and scalars, respectively, i.e.

$$Y_{11}^* = RY_{11}R^T, \quad Y_{14}^* = RY_{14}, \quad Y_{44}^* = Y_{44}. \tag{4.16}$$

These are extensions to the corresponding elasticity theorems of Ting (1982), and a shorter proof is given in Appendix A.

A bimaterial matrix is defined as

$$H = Y_1 + \bar{Y}_2, \tag{4.17}$$

where the overbar indicates complex conjugation. Hereafter the subscripts 1 and 2 attached to matrices and vectors distinguish the two materials; this notation should not cause confusion if one notes the context in which it appears. H maintains all the properties of Y listed above.

The general solution involves four analytic functions, each depending on its own complex variable. Following the one-complex-variable approach introduced in Suo (1990), we consider a column of a single variable defined as

$$\mathbf{f}(z) = \{f_1(z), f_2(z), f_3(z), f_4(z)\}, \quad z = x + \zeta y, \quad \mathrm{Im}(\zeta) > 0. \tag{4.18}$$

The solution to any given boundary value problem can be given in terms of such a column, regardless of the precise value of ζ. To compute the field quantities from (4.6) and (4.7), one must substitute z_1, z_2, z_3 or z_4 for each component function. This approach combines standard matrix operations with the techniques of analytic functions of *one* variable, and thus bypasses some complexities arising from the use of four complex variables. Of particular importance are the quantities on the x-axis:

$$\mathbf{v}(x) = \{u_j, \phi\} = A\mathbf{f}(x) + \bar{A}\bar{\mathbf{f}}(x), \tag{4.19}$$

$$\mathbf{t}(x) = \{\sigma_{2j}, D_2\} = B\mathbf{f}'(x) + \bar{B}\bar{\mathbf{f}}'(x). \tag{4.20}$$

The general solution has the same structure as the corresponding anisotropic elasticity problem. Indeed, results in the following two sections were initially anticipated from the corresponding elasticity solutions given in Willis (1971) and Suo (1990).

We should remark that the eigenvalue problem (4.5) can be recast in an alternative form using an eight-dimensional framework due to Barnett and Lothe (1975). Indeed the study by Kuo and Barnett (1991) of interfacial cracks in bonded piezoelectrics uses the eight-dimensional formalism rather than the four-dimensional framework of this section.

5. Cracks in Piezoelectrics

Results in this section apply to cracks in homogeneous piezoelectrics, and interface cracks for piezoelectric bimaterials having sufficient symmetry leading to a real valued H. Such interfaces have been discussed by Qu and Bassani (1989) for elastic materials.

5.1. *Crack tip field*

We begin with an asymptotic problem. A semi-infinite crack lies on the interface $y = 0$ between two half spaces, material 1 above, and 2 below. The crack tip coincides with the origin $x = 0$; the bonded interface is on $x > 0$. Denote L as the cracked

segment. Assume the bond is perfect, so that the displacement and potential are continuous across the bonded segment:

$$\mathbf{v}_1(x) = \mathbf{v}_2(x), \quad x \notin L. \tag{5.1}$$

There is no external charge or traction on the bonded interface, so that

$$\mathbf{t}_1(x) = \mathbf{t}_2(x), \quad x \notin L. \tag{5.2}$$

As discussed in Section 1, ferroelectric ceramics are much stiffer and more permittant than the environment, so that stress and electric induction outside of the ceramic are assumed to be negligible, and, in addition, there is no charge or traction on the crack faces. Thus,

$$\mathbf{t}_1(x) = \mathbf{t}_2(x) = 0, \quad x \in L. \tag{5.3}$$

Furthermore, the field vanishes far away from the crack tip, i.e. $\mathbf{f}'(z) = o(z^0)$ as z goes to infinity. This is an eigenvalue problem: no length or load is involved.

Let the columns defined in (4.18) be $\mathbf{f}_1(z)$ and $\mathbf{f}_2(z)$ for the two blocks. The continuity of $\mathbf{t}(x)$ across the x-axis, *both* the bonded and cracked segments, requires that

$$B_1\mathbf{f}_1'(x) + \bar{B}_1\bar{\mathbf{f}}_1'(x) = B_2\mathbf{f}_2'(x) + \bar{B}_2\bar{\mathbf{f}}_2'(x), \quad -\infty < x < +\infty. \tag{5.4}$$

The above is rearranged in the form

$$B_1\mathbf{f}_1'(x) - \bar{B}_2\bar{\mathbf{f}}_2'(x) = B_2\mathbf{f}_2'(x) - \bar{B}_1\bar{\mathbf{f}}_1'(x), \quad -\infty < x < +\infty. \tag{5.5}$$

The left-hand side of (5.5) is the boundary value of a function analytic in the upper half-plane, and the right-hand side is the boundary value of another function analytic in the lower half-plane. Hence, both functions can be analytically continued into the entire plane. Since both vanish at infinity to conform to a zero far field, they must vanish at any $z = x + \zeta y (\text{Im}\ \zeta > 0)$. Thus,

$$B_1\mathbf{f}_1'(z) = \bar{B}_2\bar{\mathbf{f}}_2'(z), \quad y > 0. \tag{5.6}$$

Define the jump across the interface

$$\mathbf{d}(x) = \mathbf{v}_1(x) - \mathbf{v}_2(x). \tag{5.7}$$

Equations (5.6) and (4.19) give

$$i\mathbf{d}'(x) = HB_1\mathbf{f}_1'(x) - \bar{H}B_2\mathbf{f}_2'(x). \tag{5.8}$$

The solution is simple if H is real, that is

$$H = \bar{H}. \tag{5.9}$$

When the crack is in a homogeneous material, H is indeed real:

$$H = Y + \bar{Y} = 2\ \text{Re}\ Y. \tag{5.10}$$

H can be real for bimaterials having certain symmetry. In the rest of this section, we assume H is real. The interfaces for which H is complex will be treated in the next section.

Continuity of the displacement across the bonded interface, as inferred from (5.8), implies that a function defined as

$$\mathbf{h}(z) = \begin{cases} B_1\mathbf{f}_1'(z), & y > 0, \\ B_2\mathbf{f}_2'(z), & y < 0 \end{cases} \tag{5.11}$$

is analytic in the entire plane except on the crack. The traction–charge boundary condition (5.3) leads to a homogeneous Hilbert problem

$$\mathbf{h}^+(x) + \mathbf{h}^-(x) = 0, \quad x \in L, \tag{5.12}$$

where superscripts + and − distinguish the boundary values when the crack is approached from above and below, respectively. The singular solution to (5.12) that gives bounded displacement and potential is

$$\mathbf{h}(z) = (8\pi z)^{-1/2}\mathbf{k}, \tag{5.13}$$

where the branch cut is along the crack line. Note that the full field is obtained once $\mathbf{h}(z)$ is determined. A few explicit results are given below.

At a distance r ahead of the crack tip

$$\{\sigma_{2j}, D_2\} = (2\pi r)^{-1/2}\mathbf{k}. \tag{5.14}$$

Since the traction and the charge are real, $\mathbf{k}$ must be real. Following Irwin's nomenclature, we write

$$\mathbf{k} = \{K_{\mathrm{II}}, K_{\mathrm{I}}, K_{\mathrm{III}}, K_{\mathrm{IV}}\}. \tag{5.15}$$

Thus the stress and the electric induction are a linear superposition of the four modes of square root singularities. At a distance r *behind* the crack tip

$$\mathbf{d}(r) = (2r/\pi)^{1/2} H\mathbf{k}. \tag{5.16}$$

The displacement jump and the voltage across the crack are asymptotically parabolas. Since, in general, H contains off-diagonal elements, a K_{IV} field will give rise to crack opening, and a K_{I} field to voltage between the crack faces.

The energy release rate can be computed by the closure integral

$$\mathscr{G} = \frac{1}{2\Lambda}\int_0^{\Lambda} \mathbf{t}^T(\Lambda - r)\mathbf{d}(r)\,\mathrm{d}r, \tag{5.17}$$

where Λ is an arbitrary length. This is consistent with the definition in Section 3, and was derived by IRWIN (1957) for cracks in elastic materials. Using (5.14) and (5.16) we obtain

$$\mathscr{G} = \tfrac{1}{4}\mathbf{k}^T H\mathbf{k}. \tag{5.18}$$

Since H is indefinite [see (4.14)], $\mathscr{G}$ can be negative for $\mathbf{k}$ with a large component K_{IV}. In deriving (5.18), the identity

$$\int_0^1 t^q(1-t)^{-q}\,\mathrm{d}t = q\pi/\sin q\pi, \quad (|\mathrm{Re}\, q| < 1) \tag{5.19}$$

has been used with $q = 1/2$.

5.2. *Full-field solutions*

Having obtained the asymptotic fields, we turn our attention to a class of boundary value problems. Consider a set of cracks on the interface, collectively denoted by L. The only applied load is the traction–charge column $\mathbf{T}(x)$ prescribed on the crack faces:

$$\mathbf{t}_1(x) = \mathbf{t}_2(x) = -\mathbf{T}(x), \quad x \in L. \tag{5.20}$$

This problem is basic: other loadings can be solved by superposition. The Hilbert problem (5.12) becomes non-homogeneous:

$$\mathbf{h}^+(x) + \mathbf{h}^-(x) = -\mathbf{T}(x), \quad x \in L. \tag{5.21}$$

This equation has many solutions. The auxiliary conditions that render a unique solution are: $\mathbf{h}(z) = o(z^0)$ as $|z| \to \infty$, $\mathbf{h}(x)$ is square root singular at the crack tips, and the net Burgers vector for every finite crack vanishes. From (5.8), the last statement leads to

$$\int_{x_a}^{x_b} [\mathbf{h}^+(x) - \mathbf{h}^-(x)]\,\mathrm{d}x = 0 \tag{5.22}$$

for a finite crack in (x_a, x_b).

Remarkably, the governing equations (5.21) and (5.22) do not involve any material constants. Thus the solution must be identical to that of a mode III crack in a homogeneous, isotropic, elastic body. The solutions to particular crack arrangements are available in handbooks. As an illustration, we consider the generalized Griffith problem: a crack of length $2a$ in an infinite piezoelectric, subjected to a uniform traction–charge column $\mathbf{T}$. The solution is

$$\int \mathbf{h}(z)\,\mathrm{d}z = \tfrac{1}{2}\mathbf{T}[(z^2 - a^2)^{1/2} - z], \tag{5.23}$$

where the branch cut for the square root coincides with the crack. The two columns, $\mathbf{f}_1$ and $\mathbf{f}_2$, are obtained from (5.23) and (5.11). The field quantities are given by (4.6) and (4.7), with z_α substituted for each component function and each material. For example, one can confirm that

$$\mathbf{t}(x) = [x(x^2 - a^2)^{-1/2} - 1]\mathbf{T}, \quad |x| > a, \tag{5.24}$$

$$\mathbf{d}(x) = (a^2 - x^2)^{1/2} H\mathbf{T}, \quad |x| < a. \tag{5.25}$$

Suppose that the traction and charge are caused by the remote fields $\{\sigma_{2f}^\infty, D_2^\infty\}$. The intensity factors are identical with the classical ones for a crack in an isotropic elastic material:

$$K_{\mathrm{II}} = \sqrt{\pi\alpha}\sigma_{21}^{\infty}, \quad K_{\mathrm{I}} = \sqrt{\pi a}\sigma_{22}^{\infty}, \quad K_{\mathrm{III}} = \sqrt{\pi a}\sigma_{23}^{\infty}, \quad K_{\mathrm{IV}} = \sqrt{\pi a}D_2^{\infty}. \tag{5.26}$$

This result is surprising because it holds for piezoelectric materials with arbitrary anisotropy. However, the simplicity is accidental rather than a rule: it only works for cracks between identical half-spaces, or for certain special bimaterials.

6. Interface Cracks

Bimaterials with complex H are examined in this section, which is the more common case for interfaces, be they dielectrics, piezoelectrics or conductors. The results in the above section up to (5.8) are still valid. Continuity of displacement across the bonded interface now requires that a function defined as

$$\mathbf{h}(z) = \begin{cases} B_1\mathbf{f}_1'(z), & y > 0, \\ H^{-1}\bar{H}B_2\mathbf{f}_2'(z), & y < 0 \end{cases} \tag{6.1}$$

be analytic in the whole plane except on the crack lines. Once $\mathbf{h}(z)$ is found, so is the full field.

6.1. *Crack tip field*

Consider the asymptotic problem first. The traction–charge-free condition (5.3) gives

$$\mathbf{h}^+(x) + \bar{H}^{-1}H\mathbf{h}^-(x) = 0, \quad x \in L. \tag{6.2}$$

This is a homogeneous Hilbert problem. A solution can be sought of the form

$$\mathbf{h}(z) = \mathbf{w}z^{-1/2+i\varepsilon}, \tag{6.3}$$

where $\mathbf{w}$ is a four-element column and ε a number, both to be determined. The branch cut coincides with the crack line, and the phase angle of z is measured from the positive x-axis. Substituting (6.3) into (6.2) gives

$$\bar{H}\mathbf{w} = e^{2\pi\varepsilon}H\mathbf{w}. \tag{6.4}$$

This is a 4×4 eigenvalue problem. The algebraic details of the solution are important for understanding the crack tip field; they are recorded in Appendix B. The four eigenpairs have the structure

$$(\varepsilon, \mathbf{w}), \quad (-\varepsilon, \bar{\mathbf{w}}), \quad (-i\kappa, \mathbf{w}_3), \quad (i\kappa, \mathbf{w}_4), \tag{6.5}$$

where ε, κ, $\mathbf{w}_3$ and $\mathbf{w}_4$ are real, but $\mathbf{w}$ is complex.

The general solution to (6.2) is then a linear combination of the four solutions of the form (6.3):

$$\mathbf{h}(z) = \frac{e^{\pi\varepsilon}Kz^{i\varepsilon}\mathbf{w} + e^{-\pi\varepsilon}\bar{\mathbf{K}}\mathbf{z}^{-i\varepsilon}\bar{\mathbf{w}}}{2\sqrt{2\pi z}\cosh\pi\varepsilon} + \frac{K_3z^{\kappa}\mathbf{w}_3 + K_4z^{-\kappa}\mathbf{w}_4}{2\sqrt{2\pi z}\cos\pi\kappa}, \tag{6.6}$$

where K is complex and K_3 and K_4 are real; they are intensity factors. The arrangement

ensures that the traction and the charge are real, and renders a simple expression for the traction–charge interface. The novel feature of (6.6) is the presence of singularities of order $r^{-1/2+\kappa}$ and $r^{-1/2-\kappa}$, which were previously found by KUO and BARNETT (1991). The latter singularity is particularly surprising because it provides a term of order $r^{-1-2\kappa}$ in the integrand of the J-integral (3.5), which appears to conflict with path-independence of the J-integral (in elasticity, the integrand has order r^{-1}). This apparent paradox will be resolved below.

It is convenient to display physical quantities in an eigenvector representation. For example, write the column $\mathbf{t}(x), x > 0$ as

$$\mathbf{t} = t\mathbf{w} + \bar{t}\bar{\mathbf{w}} + t_3\mathbf{w}_3 + t_4\mathbf{w}_4. \tag{6.7}$$

Because $\mathbf{t}$ is real, the components for $\mathbf{w}$ and $\bar{\mathbf{w}}$ must be complex conjugate, and t_3 and t_4 are real. Consequently, the $\mathbf{t}$-column in the interface a distance r ahead of the crack tip has three components: one is in the plane spanned by Re [$\mathbf{w}$] and Im [$\mathbf{w}$], the other two are along the $\mathbf{w}_3$- and $\mathbf{w}_4$-directions. These components vary with r according to

$$t = \frac{Kr^{i\varepsilon}}{\sqrt{2\pi r}}, \quad t_3 = \frac{K_3 r^{\kappa}}{\sqrt{2\pi r}}, \quad t_4 = \frac{K_4 r^{-\kappa}}{\sqrt{2\pi r}}. \tag{6.8}$$

The above may be taken as defining equations for the intensity factors. As $r \to 0$, the component t rotates in the plane spanned by Re [$\mathbf{w}$] and Im [$\mathbf{w}$]. This is clearly the analog of the corresponding result for isotropic elastic bimaterial, where $t \equiv \sigma_{yy} + i\sigma_{xy}$.

The jump $\mathbf{d}$ a distance r behind the tip is

$$\mathbf{d} = (H+\bar{H})\sqrt{\frac{r}{2\pi}}\left[\frac{Kr^{i\varepsilon}\mathbf{w}}{(1+2i\varepsilon)\cosh \pi\varepsilon} + \frac{\bar{K}r^{-i\varepsilon}\bar{\mathbf{w}}}{(1-2i\varepsilon)\cosh \pi\varepsilon} + \frac{K_3 r^{\kappa}\mathbf{w}_3}{(1+2\kappa)\cos \pi\kappa} + \frac{K_4 r^{-\kappa}\mathbf{w}_4}{(1-2\kappa)\cos \pi\kappa}\right]. \tag{6.9}$$

Substituting the above crack tip field into the closure integral (5.17) gives

$$\mathcal{G} = \frac{\bar{\mathbf{w}}^T(\mathbf{H}+\bar{\mathbf{H}})\mathbf{w}}{4\cosh^2 \pi\varepsilon}|K|^2 + \frac{\mathbf{w}_3^T(\mathbf{H}+\bar{\mathbf{H}})\mathbf{w}_4}{4\cos^2 \pi\kappa} K_3 K_4. \tag{6.10}$$

In deriving this, we have used the orthogonality described in Appendix B, and the identity (5.19) with $q = 1/2 \pm \kappa,\ 1/2 \pm i\varepsilon$. The paradox related to the J-integral is resolved by this result, i.e., $J = \mathcal{G}$, just as in the case of elasticity, so that J is indeed finite and the term of order $r^{-1-2\kappa}$ in the integrand must integrate to zero. This is reflected in the orthogonality $\mathbf{w}_4^T H \mathbf{w}_4 = 0$ which, had it not been satisfied, would have introduced into the closure integral (5.17) a term of order $r^{-1-2\kappa}$, with the consequence that a finite $\mathcal{G}$ could not have been defined.

No normalization has yet been assigned to the eigenvectors. A different normalization changes K_3 and K_4 by real factors, and K by a complex factor.

6.2. *Full-field solutions*

Now consider the boundary value problems in Section 5.2 for complex H. The Hilbert problem analogous to (5.21) is

$$\mathbf{h}^+(x)+\bar{H}^{-1}H\mathbf{h}^-(x) = -\mathbf{T}(x), \quad x\in L. \tag{6.11}$$

Writing the above equation in its components using the eigenvector representation,

$$\mathbf{h} = h_1\mathbf{w}+h_2\bar{\mathbf{w}}+h_3\mathbf{w}_3+h_4\mathbf{w}_4, \quad \mathbf{T} = T\mathbf{w}+\bar{T}\bar{\mathbf{w}}+T_3\mathbf{w}_3+T_4\mathbf{w}_4, \tag{6.12}$$

one obtains the decoupled equations

$$\begin{aligned} h_1^+ + e^{-2\pi\varepsilon}h_1^- &= -T, \qquad h_2^+ + e^{+2\pi\varepsilon}h_2^- = -\bar{T}, \\ h_3^+ + e^{2\pi i\kappa}h_3^- &= -T_3, \quad h_4^+ + e^{-2\pi i\kappa}h_4^- = -T_4. \end{aligned} \tag{6.13}$$

Furthermore, since they contain no explicit material dependence besides ε and κ, their solutions must be identical to those for isotropic elastic bimaterials. One can derive the solution using the method of analytic functions or from the known solutions for isotropic elastic bimaterials.

As an illustration, consider the generalized Griffith problem with a crack of length $2a$ on the interface between two half-spaces of piezoelectrics. Consulting ENGLAND (1965), where the corresponding elasticity problem was solved, we obtain

$$\begin{aligned} \int h_1(z)\,dz &= \frac{T}{1+e^{-2\pi\varepsilon}}\left[\left(\frac{z-a}{z+a}\right)^{i\varepsilon}(z^2-a^2)^{1/2}-z\right], \\ \int h_3(z)\,dz &= \frac{T_3}{1+e^{2\pi i\kappa}}\left[\left(\frac{z-a}{z+a}\right)^{\kappa}(z^2-a^2)^{1/2}-z\right], \end{aligned} \tag{6.14}$$

where h_2 and h_4 are omitted, for they can be obtained by substitutions. The intensity factors are

$$\begin{aligned} K &= T(1+2i\varepsilon)\cosh(\pi\varepsilon)(\pi a)^{1/2}(2a)^{-i\varepsilon}, \\ K_3 &= T_3(1+2\kappa)\cos(\pi\kappa)(\pi a)^{1/2}(2a)^{-\kappa}. \end{aligned} \tag{6.15}$$

Without re-solving any problems, one can write down solutions for many cracks on the interface between half spaces of piezoelectrics, provided the corresponding solutions for isotropic elastic bimaterials are known.

7. FRACTURE MECHANICS

7.1. *Unpoled ferroelectric ceramics*

Unpoled $BaTiO_3$ makes good capacitors due to its large permittivity. The polycrystalline, multi-domain structure cancels the macroscopic piezoelectricity. This special class of materials is ideal for theoretical study since it has a simple macroscopic field, yet still retains the essential features of ferroelectric ceramics. In Section 5, we have established that the piezoelectric field around the crack tip is square root singular and linear in four intensity factors. But what is the crack tip? Or what does the singularity mean physically? The assumed material linearity cannot hold at the crack tip. Specifically, ferroelectric ceramics undergo hysteresis under sufficiently high loading. Furthermore, down to a small scale many other features, such as the presence of

grains and domains, will invalidate the solution. Consequently, the solution given above is only correct at some distance away from the crack tip.

Because of the square root singularity, for large specimens, an annulus exists, smaller than the specimen size but larger than the crack process zone, in which the field is described by the singular field of Section 5. This so-called K-annulus is parameterized by the four intensity factors: any other information will be lost in the communication between the macroscopic loading and microscopic process. Consequently, the fracture criterion can be written in terms of the four intensity factors. Most fracture tests have been conducted with specimens under symmetric loading, such as double-cantilever-beams in Fig. 2. This will in general produce both mode I and mode IV fields at the crack tip. The general results in Section 5 are specialized to this case below, with matrix Y given by (A2).

The stress and the electric induction are square root singular as the crack tip is approached. Let the crack plane be normal to the z-axis. The intensity factors K_{I} and K_{IV} are defined such that, at a distance r ahead of the crack tip,

$$\sigma_{zz} = \frac{K_{\mathrm{I}}}{\sqrt{2\pi r}}, \quad D_z = \frac{K_{\mathrm{IV}}}{\sqrt{2\pi r}}. \tag{7.1}$$

The crack separation and voltage at a distance r behind the crack tip are given by

$$\Delta u_z = \frac{4(1-\nu)}{\mu}\sqrt{\frac{r}{2\pi}}\,K_{\mathrm{I}}, \quad \Delta\phi = -\frac{4}{\varepsilon}\sqrt{\frac{r}{2\pi}}\,K_{\mathrm{IV}}, \tag{7.2}$$

where ν is the Poisson's ratio, μ the shear modulus and ε the permittivity; they are macroscopic average quantities of the polycrystalline ceramics. The Irwin-type relation connecting $\mathcal{G}$ and the intensity factors is

$$\mathcal{G} = \frac{2(1-\nu)}{\mu}K_{\mathrm{I}}^2 - \frac{1}{2\varepsilon}K_{\mathrm{IV}}^2. \tag{7.3}$$

Under static loading, the fracture criterion should be of the form

$$\mathcal{G} = \Gamma\left(\sqrt{\mu/\varepsilon}K_{\mathrm{IV}}/K_{\mathrm{I}}\right), \tag{7.4}$$

where Γ is the fracture energy depending on the mixity of modes I and IV. Whether K_{IV} will influence Γ depends on the magnitude of the dimensionless mixity, and on the crack tip process. In particular, the hysteresis strain associated with the domain switching as the crack grows is likely to play an important role.

Under cyclic loading, a ferroelectric usually is subjected to low load, but the field concentrated at the crack tip generates hysteresis loops locally so that fatigue is possible, as observed experimentally by WINZER *et al.* (1989). No systematic experiments or modeling have been done in this area. The present work would allow fatigue crack growth due to the small-scale hysteresis to be evaluated using the approach for low-stress high-cycle fatigue crack growth in metals. It is anticipated that experiments analogous to those described in PARIS and ERDOGAN (1963) for metal fatigue would establish Paris-type laws for ferroelectrics. Specifically, the crack extension per cycle, $\mathrm{d}a/\mathrm{d}N$, must be a function of the loading range, i.e.

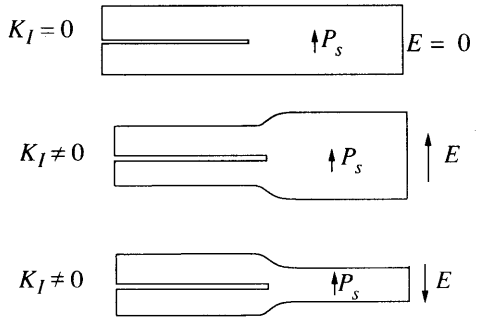

FIG. 4. For a double-cantilever-beam, a mixed field of modes I and IV is induced by the voltage alone. When E is parallel with P_s, the uncracked portion undergoes a piezoelectric expansion along E, but the cracked portion remains unchanged. The strain misfit causes stress ahead of the crack tip, and thus $K_I \neq 0$.

$$da/dN = f(\Delta K_I, \Delta K_{IV}). \tag{7.5}$$

This relation characterizes a material property, which is independent of the geometry of the samples being tested.

7.2. *Poled ferroelectric ceramics*

The additional complexity due to piezoelectricity can be illustrated by a special case of much practical significance: cracks in a plane normal to the poling axis of the poled ceramics. The relevant algebraic details are discussed in Appendix C. Most fracture tests have been conducted with specimens under symmetric mechanical loading, such as double-cantilever-beams in Fig. 2. This will in general produce both mode I and mode IV fields at the crack tip. The intensity factors are still defined by (7.1). The crack separation and voltage at a distance r behind the crack tip are given by

$$\Delta u_z = 4\sqrt{\frac{r}{2\pi}}\left(\frac{K_I}{C_T} + \frac{K_{IV}}{e}\right), \quad \Delta\phi = 4\sqrt{\frac{r}{2\pi}}\left(-\frac{K_{IV}}{\varepsilon} + \frac{K_I}{e}\right), \tag{7.6}$$

where C_T, ε and e are effective moduli determined by the procedure in Appendix C. The Irwin-type relation connecting $\mathcal{G}$ and the intensity factors is

$$\mathcal{G} = \frac{1}{2C_T}K_I^2 - \frac{1}{2\varepsilon}K_{IV}^2 + \frac{1}{e}K_I K_{IV}. \tag{7.7}$$

Although the macroscopic field is much more involved in this case, the fracture mechanisms are expected to be qualitatively similar to those of unpoled materials.

As illustrated in Fig. 4, the double-cantilever-beam has a mode I component under electric loading alone. This can be appreciated by noting that the material far behind the crack tip is not loaded, and the strain induced by the voltage ahead of the tip causes the stress intensity. However, finite element analysis by HE *et al.* (1991) indicates that K_I due to V is typically small.

7.3. *Interface debonding*

Debonding at electrodes and other interfaces has been identified to be a major failure mode in piezoelectric and electrostrictive actuators (WINZER *et al.*, 1989), although no systematic testing and modeling have been carried out. We believe that concepts used in elastic interface fracture mechanics are applicable for such a study [see RICE (1988) and SUO (1991) for brief reviews]. A more extensive discussion on the fracture of layered materials has been presented by HUTCHINSON and SUO (1992).

In Section 6 we found that the crack tip field is linear in three intensity factors, one complex and two real, of different dimensions. Interfacial fracture in general should be of the mixed-mode type. The mode mixity must be chosen to reflect the state at the tip. A length scale, $\hat{L}$, representative of the process zone size, may be identified, and the mode mixity can be defined by the dimensionless ratios

$$\mathrm{Im}\,(\hat{L}^{i\varepsilon}K)/|K|, \quad \hat{L}^{\kappa}K_3/|K|, \quad \hat{L}^{-\kappa}K_4/|K|, \tag{7.8}$$

the fracture toughness depending on these mixities. The experimental determination of the mixed-mode toughness presents a formidable task. Simplifications are possible for special crack orientations and loading conditions. For example, for unpoled capacitor materials, the mechanical and the electrical fields are decoupled at the macroscopic level, so that only K_{IV} defined as in (7.1) is present under electrical loading. This fact simplifies the fracture mechanics for the ceramic–metal interfaces.

8. CONCLUDING REMARKS

Microcracking, fatigue and fracture are among the properties that limit the use of ferroelectric ceramics as large strain actuators. A fracture mechanics theory is developed here to evaluate static toughness and fatigue crack growth for ferroelectric ceramics under small-scale hysteresis. It is likely that various toughening concepts for structural ceramics may find their electrical counterparts, so that ferroelectric materials may be engineered to exhibit superior performance. Future necessary work will include calibrating electromechanical fracture specimens using finite elements, failure testing under static and cyclic loads, modeling of fracture processes at the crack tip to understand the role of ferroelectric hysteresis and accounting for the presence of a conducting fluid, and analyzing typical structures such as piezoelectric films and multilayer actuators.

ACKNOWLEDGEMENTS

ZS is funded by ONR/URI contract N-0-0014-86-K-0753 and NSF grant MSS-9011571.

REFERENCES

BARNETT, D. M. and LOTHE, J. 1975 *Physica Status Solidi (b)* **67,** 105.
CHUNG, H.-T., SHIN, B.-C. and KIM, H.-G. 1989 *J. Am. Ceram. Soc.* **72,** 327.

DEEG, W. F. J.	1980	Ph.D. Thesis, Stanford University.
ENGLAND, A. H.	1965	*J. appl. Mech.* **32,** 400.
ESHELBY, J. D., READ, W. T. and SHOCKLEY, W.	1953	*Acta metall.* **1,** 251.
FATUZZO, E. and MERZ, W. J.	1967	*Ferroelectricity*. North Hollland, New York.
FEYNMAN, R. P., LEIGHTON, R. B. and SANDS, M.	1964	*Lectures on Physics*, Vol. 2, p. 10-9. Addison–Wesley, Reading, MA.
FREIMAN, S. W. and POHANKA, R. C.	1989	*J. Am. Ceram. Soc.* **72,** 2258.
HAYASHI, M., IMAIZUMI, S. and ABE, R.	1964	*Jap. J. appl. Phys.* **3,** 637.
HE, M.-Y., SUO, Z., MCMEEKING, R. M. and EVANS, A. G.	1991	Manuscript in preparation.
HUTCHINSON, J. W. and SUO, Z.	1992	*Adv. appl. Mech.* **29** (in press).
IRWIN, G. R.	1957	*J. appl. Mech.* **24,** 361.
JAFFE, B., COOK, W. R., JR. and JAFFE, H.	1971	*Piezoelectric Ceramics*. Academic Press, London.
KUO, C.-M. and BARNETT, D. M.	1991	In *Modern Theory of Anisotropic Elasticity and Applications* (edited by J. J. WU, T. C. T. TING and D. M. BARNETT), pp. 33–50. SIAM Proceedings Series, Philadelphia, PA.
LOTHE, J. and BARNETT, D. M.	1975	*J. appl. Phys.* **47,** 1799.
MCMEEKING, R. M.	1987	*J. appl. Phys.* **62,** 3116.
MCMEEKING, R. M.	1989	*J. appl. Math. Phys.* **40,** 615.
MCMEEKING, R. M.	1990	*Int. J. Engng Sci.* **28,** 605.
MIKHAILOV, G. K. and PARTON, V. Z.	1990	*Electromagnetoelasticity*. Hemisphere, New York.
PAK, Y. E.	1990	*J. appl. Mech.* **57,** 647.
PAN, W. Y., DAM, C. Q., ZHANG, Q. M. and CROSS, L. E.	1989	*J. appl. Phys.* **66,** 6014.
PARIS, P. C. and ERDOGAN, F.	1963	*J. Basic Engng* **85,** 528.
PARTON, V. Z.	1976	*Acta astronaut.* **3,** 671.
POHANKA, R. C. and SMITH, P. L.	1987	In *Electronic Ceramics* (edited by L. M. LEVINSON), pp. 45–146. Marcel Dekker, New York.
QU, J. and BASSANI, J. L.	1989	*J. Mech. Phys. Solids* **37,** 417.
RICE, J. R.	1968	*J. appl. Mech.* **35,** 379.
RICE, J. R.	1988	*J. appl. Mech.* **55,** 98.
SHINDO, Y., OZAWA, E. and NOWACKI, J. P.	1990	*Appl. Electromagn. Mater.* **1,** 77.
SOSA, H. A. and PARK, Y. E.	1990	*Int. J. Solids Struct.* **26,** 1.
STROH, A. N.	1958	*Phi. Mag.* **7,** 625.
SUO, Z.	1990	*Proc. R. Soc.* **A427,** 331.
SUO, Z.	1991	*Scr. metall. mater.* **25,** 1011.
SUO, Z.	1992	Submitted for publication.
TING, T. C. T.	1982	*Int. J. Solids Struct.* **18,** 139.
TING, T. C. T.	1986	*Int. J. Solids Struct.* **22,** 965.
WILLIS, J. R.	1971	*J. Mech. Phys. Solids* **19,** 353.
WINZER, S. R., SHANKAR, N. and RITTER, A. P.	1989	*J. Am. Ceram. Soc.* **72,** 2246.

APPENDIX A

A few algebraic theorems of the complex variable representation are documented here. First, following the method used by ESHELBY *et al.* (1953) for the elasticity problem, we prove that

the eigenvalues p of (4.5) are complex. Multiply the first equation in (4.5) by a_j and sum over j, and multiply the second by a_4; the difference of the two results is

$$(C_{\alpha jr\beta}a_r a_j + \varepsilon_{\alpha\beta}a_4^2)\zeta_\alpha\zeta_\beta = 0. \tag{A1}$$

If an eigenvalue p is real, the associated eigenvector $\mathbf{a}$ can be chosen as real, and, therefore, with C and ε positive definite, the left-hand side of (A1) must be positive. Hence, by contradiction p cannot be real.

Next consider the matrix Y defined by (4.11). For isotropic, non-piezoelectric dielectrics, the in-plane displacements, the anti-plane displacement, and the electric potential decouple. Unpoled ferroelectric materials belong to this class. The general representation (4.6) fails because of the degeneracy associated with such symmetry, but Y can be found by a limiting process which gives

$$Y = \begin{bmatrix} \dfrac{1-v}{\mu} & i\left(\dfrac{1-2v}{2\mu}\right) & 0 & 0 \\ -i\left(\dfrac{1-2v}{2\mu}\right) & \dfrac{1-v}{\mu} & 0 & 0 \\ 0 & 0 & \dfrac{1}{\mu} & 0 \\ 0 & 0 & 0 & -\dfrac{1}{\varepsilon} \end{bmatrix}, \tag{A2}$$

where v is the Poisson's ratio, μ the shear modulus and ε the permittivity. Note that conductors can be treated by setting $\varepsilon = \infty$. Several properties shown in this special case are general to all piezoelectrics. They have been mentioned in the text and their proofs are outlined below.

We show that Y is Hermitian. The proof parallels that of STROH (1958) for the elasticity problem. From (4.8) we have

$$\bar{p}^{(2)}\bar{\mathbf{a}}^{(2)}\cdot\mathbf{b}^{(1)} = \{C_{2jr\beta}\bar{a}_j^{(2)}a_r^{(1)} + e_{\beta j2}\bar{a}_j^{(2)}a_4^{(1)} - \varepsilon_{2\beta}\bar{a}_4^{(2)}a_4^{(1)} + e_{2r\beta}\bar{a}_4^{(2)}a_r^{(1)}\}\bar{\zeta}_2^{(2)}\zeta_\beta^{(1)}, \tag{A3}$$

and from (4.9)

$$p^{(1)}\bar{\mathbf{a}}^{(2)}\cdot\mathbf{b}^{(1)} = -\{C_{1jr\beta}\bar{a}_j^{(2)}a_r^{(1)} + e_{\beta j1}\bar{a}_j^{(2)}a_4^{(1)} - \varepsilon_{1\beta}\bar{a}_4^{(2)}a_4^{(1)} + e_{1r\beta}\bar{a}_4^{(2)}a_r^{(1)}\}\bar{\zeta}_1^{(2)}\zeta_\beta^{(1)}. \tag{A4}$$

Subtracting these two equations,

$$(\bar{p}^{(2)} - p^{(1)})\bar{\mathbf{a}}^{(2)}\cdot\mathbf{b}^{(1)} = \{C_{\alpha jr\beta}\bar{a}_j^{(2)}a_r^{(1)} + (e_{\beta j\alpha} + e_{\alpha j\beta})(\bar{a}_j^{(2)}a_4^{(1)} + \bar{a}_4^{(2)}a_j^{(1)}) - \varepsilon_{\alpha\beta}\bar{a}_4^{(2)}a_4^{(1)}\}\bar{\zeta}_\alpha^{(2)}\zeta_\beta^{(1)}. \tag{A5}$$

Now the right-hand side has the Hermitian symmetry for indices (1) and (2), and so the left-hand side must also; that is,

$$(\bar{p}^{(2)} - p^{(1)})\bar{\mathbf{a}}^{(2)}\cdot\mathbf{b}^{(1)} = (p^{(1)} - \bar{p}^{(2)})\mathbf{a}^{(1)}\cdot\bar{\mathbf{b}}^{(2)}, \tag{A6}$$

or, since $(\bar{p}^{(2)} - p^{(1)})$ has negative imaginary part and so is not zero,

$$\bar{\mathbf{a}}^{(2)}\cdot\mathbf{b}^{(1)} = -\mathbf{a}^{(1)}\cdot\bar{\mathbf{b}}^{(2)}. \tag{A7}$$

From the definition (4.11) of Y, the above implies that

$$Y^T = \bar{Y}, \tag{A8}$$

that is, Y is Hermitian. Only the reciprocal symmetry in (2.10) is invoked in the proof.

Now consider the coordinate rotation (4.15). Since C, e and ε are tensors, from (4.5) $\{\zeta_1, \zeta_2\}$ transforms like a vector, $\{a_1, a_2, a_3\}$ a vector and a_4 a scalar. Specifically,

$$\begin{bmatrix} \zeta_1^* \\ \zeta_2^* \end{bmatrix} = \begin{bmatrix} \cos\theta & \sin\theta \\ -\sin\theta & \cos\theta \end{bmatrix} \begin{bmatrix} \zeta_1 \\ \zeta_2 \end{bmatrix}. \tag{A9}$$

With the identification that $p = \zeta_2/\zeta_1$ and $p^* = \zeta_2^*/\zeta_1^*$, one obtains that

$$p^* = \frac{p\cos\theta - \sin\theta}{p\sin\theta + \cos\theta}. \tag{A10}$$

Equation (4.8) implies that $\{b_1, b_2, b_3\}$ transforms like a vector and b_4 a scalar. Define

$$\tilde{R} = \begin{bmatrix} R & 0 \\ 0 & 1 \end{bmatrix} = \begin{bmatrix} \cos\theta & \sin\theta & 0 & 0 \\ -\sin\theta & \cos\theta & 0 & 0 \\ 0 & 0 & 1 & 0 \\ 0 & 0 & 0 & 1 \end{bmatrix}. \tag{A11}$$

The transformation can be summarized as

$$A^* = \tilde{R}A, \quad B^* = \tilde{R}B. \tag{A12}$$

Note that $\tilde{R}^{-1} = \tilde{R}^T$, and (4.11) implies

$$Y^* = \tilde{R}Y\tilde{R}^T. \tag{A13}$$

This completes the proof of (4.16).

APPENDIX B

The structure of the eigenvalue problem (6.4) is discussed here. The parameter ε satisfies

$$\| \bar{H} - e^{2\pi\varepsilon} H \| = 0. \tag{B1}$$

Since H is Hermitian, the transpose of (B1) is

$$\| H - e^{2\pi\varepsilon} \bar{H} \| = 0. \tag{B2}$$

Also, by complex conjugation,

$$\| H - e^{2\pi\bar{\varepsilon}} \bar{H} \| = 0. \tag{B3}$$

It follows that, if ε satisfies (B1), then so do $-\varepsilon$, $\bar{\varepsilon}$ and $-\bar{\varepsilon}$.

To make further progress, write H in its real and imaginary parts:

$$H = D + iW, \tag{B4}$$

where D is real and symmetric and W is real and antisymmetric; in this context the symbols have nothing to do with the electric induction or energy used in the main text. Equation (6.4) becomes

$$D^{-1}W\mathbf{w} = -i\beta\mathbf{w}, \tag{B5}$$

where

$$\beta = -\tanh(\pi\varepsilon), \quad \text{or} \quad \varepsilon = \frac{1}{2\pi}\ln\frac{1-\beta}{1+\beta}. \tag{B6}$$

From the observation for ε made above, if β is an eigenvalue, so are $-\beta$, $\bar{\beta}$ and $-\bar{\beta}$. It follows that (B1), written in terms of β,

$$\| D^{-1}W + i\beta I \| = 0, \tag{B7}$$

must have the form

$$\beta^4 + 2b\beta^2 + c = 0, \tag{B8}$$

where

$$b = \tfrac{1}{4}\,\mathrm{tr}\,[(D^{-1}W)^2], \quad c = \|D^{-1}W\|. \tag{B9}$$

The above were originally presented by Kuo and Barnett at a workshop, and they also gave possible sets of roots to (B8), which lead to several different crack tip singularity structures.

Since their initial presentation, the present writers have realized that only one set of the roots to (B8) is physically admissible because c is restricted as follows. Observe that $\|W\| \geqslant 0$, a property of any antisymmeric matrix of even order, and $\|D\| < 0$, a consequence of (4.14), so that

$$c \leqslant 0. \tag{B10}$$

The roots of (B8) can therefore be expressed as

$$\beta_{1,2} = \pm[(b^2-c)^{1/2}-b]^{1/2}, \quad \beta_{3,4} = \pm i[(b^2-c)^{1/2}+b]^{1/2}. \tag{B11}$$

Thus, one pair is real and the other is purely imaginary. In the notation of the body of the text

$$\varepsilon = \frac{1}{\pi}\tanh^{-1}[(b^2-c)^{1/2}-b]^{1/2}, \quad \kappa = \frac{1}{\pi}\tan^{-1}[(b^2-c)^{1/2}+b]^{1/2}. \tag{B12}$$

These results have been included in KUO and BARNETT (1991). Their numerical results indicate that ε and κ are very small for several piezoelectric bicrystals.

The associated eigenvectors satisfy

$$\bar{H}\mathbf{w} = e^{2\pi\varepsilon}H\mathbf{w}, \quad \bar{H}\bar{\mathbf{w}} = e^{-2\pi\varepsilon}H\bar{\mathbf{w}}, \quad \bar{H}\mathbf{w}_3 = e^{-2\pi i\kappa}H\mathbf{w}_3, \quad \bar{H}\mathbf{w}_4 = e^{2\pi i\kappa}H\mathbf{w}_4. \tag{B13}$$

It can be confirmed that $\mathbf{w}$ is complex but $\mathbf{w}_3$ and $\mathbf{w}_4$ are real, satisfying the orthogonality relations

$$\begin{bmatrix} \bar{\mathbf{w}}^T \\ \mathbf{w}^T \\ \mathbf{w}_3^T \\ \mathbf{w}_4^T \end{bmatrix} H[\mathbf{w}, \bar{\mathbf{w}}, \mathbf{w}_3, \mathbf{w}_4] = \begin{bmatrix} \bar{\mathbf{w}}^T H\mathbf{w} & 0 & 0 & 0 \\ 0 & \mathbf{w}^T H\bar{\mathbf{w}} & 0 & 0 \\ 0 & 0 & 0 & \mathbf{w}_3^T H\mathbf{w}_4 \\ 0 & 0 & \mathbf{w}_4^T H\mathbf{w}_3 & 0 \end{bmatrix}. \tag{B14}$$

Under a rotation of the interface but with the relative orientation of the two half-spaces fixed, H transforms according to

$$H^* = \tilde{R}H\tilde{R}^T, \tag{B15}$$

where $\tilde{R}$ is defined by (A11). Consequently, the eigenvalues ε and κ are invariant under such a rotation, and the eigenvectors transform according to

$$\mathbf{w}^* = \tilde{R}\mathbf{w}. \tag{B16}$$

These can be verified directly by substituting (B15) into (B1) and (6.4). TING (1986) observed similar results for elastic materials.

APPENDIX C

In the text, the crack problem has been solved in the sense that only algebraic operations remain to obtain explicit results. In general, Stroh's eigenvalue problem must be solved numerically. Here explicit algebraic results are given for a class of materials of practical significance: the poled ceramics. The constitutive equation has transverse symmetry around the poling axis (axis-3):

$$\begin{bmatrix}\sigma_{11}\\ \sigma_{22}\\ \sigma_{33}\\ \sigma_{23}\\ \sigma_{13}\\ \sigma_{12}\end{bmatrix}=\begin{bmatrix}c_{11} & c_{12} & c_{13} & 0 & 0 & 0\\ c_{12} & c_{11} & c_{13} & 0 & 0 & 0\\ c_{13} & c_{13} & c_{33} & 0 & 0 & 0\\ 0 & 0 & 0 & c_{44} & 0 & 0\\ 0 & 0 & 0 & 0 & c_{44} & 0\\ 0 & 0 & 0 & 0 & 0 & \frac{1}{2}(c_{11}-c_{12})\end{bmatrix}\begin{bmatrix}\gamma_{11}\\ \gamma_{22}\\ \gamma_{33}\\ 2\gamma_{23}\\ 2\gamma_{13}\\ 2\gamma_{12}\end{bmatrix}-\begin{bmatrix}0 & 0 & e_{31}\\ 0 & 0 & e_{31}\\ 0 & 0 & e_{33}\\ 0 & e_{15} & 0\\ e_{15} & 0 & 0\\ 0 & 0 & 0\end{bmatrix}\begin{bmatrix}E_1\\ E_2\\ E_3\end{bmatrix}, \tag{C1}$$

$$\begin{bmatrix}D_1\\ D_2\\ D_3\end{bmatrix}=\begin{bmatrix}0 & 0 & 0 & 0 & e_{15} & 0\\ 0 & 0 & 0 & e_{15} & 0 & 0\\ e_{31} & e_{31} & e_{33} & 0 & 0 & 0\end{bmatrix}\begin{bmatrix}\gamma_{11}\\ \gamma_{22}\\ \gamma_{33}\\ 2\gamma_{23}\\ 2\gamma_{13}\\ 2\gamma_{12}\end{bmatrix}+\begin{bmatrix}\varepsilon_{11} & 0 & 0\\ 0 & \varepsilon_{11} & 0\\ 0 & 0 & \varepsilon_{33}\end{bmatrix}\begin{bmatrix}E_1\\ E_2\\ E_3\end{bmatrix}. \tag{C2}$$

(i) Crack front coincides with the poling axis.

This case has been studied by PAK (1990). The (x, y)-plane coincides with the isotropic $(1,2)$-plane. The in-plane deformation (u_x, u_y) is decoupled from the anti-plane deformation and the potential (u_z, ϕ). The former is identical with the elasticity problem. We focus on the latter.

The complex representation given by Pak is

$$u_z = 2\,\mathrm{Re}[f_1(z)], \quad \phi = 2\,\mathrm{Re}[f_2(z)], \quad z = x+iy. \tag{C3}$$

The two characteristic roots are identical, $p_1 = p_2 = i$. Consistent with the notation of this paper, we write

$$A=\begin{bmatrix}1 & 0\\ 0 & 1\end{bmatrix}, \quad B=i\begin{bmatrix}c_{44} & e_{15}\\ e_{15} & -\varepsilon_{11}\end{bmatrix}. \tag{C4}$$

The matrix Y is then

$$Y=\frac{1}{1+k}\begin{bmatrix}c_{44}^{-1} & ke_{15}^{-1}\\ ke_{15}^{-1} & -\varepsilon_{11}^{-1}\end{bmatrix}, \quad k=e_{15}^2/(c_{44}\varepsilon_{11}). \tag{C5}$$

This is the lower right-hand block of the 4×4 matrix. The upper left-hand block is identical to that in (A2).

The complete solution is given explicitly in the text. In particular, for a crack tip in a homogeneous material,

$$\mathcal{G}=\frac{1-\nu}{2\mu}(K_{\mathrm{II}}^2+K_{\mathrm{III}}^2)+\frac{1}{2(1+k)}\left[\frac{K_{\mathrm{III}}^2}{c_{44}}-\frac{K_{\mathrm{IV}}^2}{\varepsilon_{11}}+2k\frac{K_{\mathrm{III}}K_{\mathrm{IV}}}{e_{15}}\right]. \tag{C6}$$

For an interface crack, the in-plane deformation contains an oscillatory singularity. But the field derived from (u_z, ϕ) remains square root singular, and, in each material, these components of the crack tip field remain the same as the homogeneous ones.

(ii) Crack plane perpendicular to the poling axis.

Now we look for field in $(1,3)$-plane, where u_y decouples from (u_x, u_z, ϕ). With u_y ignored, the characteristic equation (4.5) becomes

$$\begin{bmatrix}(c_{11}+c_{44}p^2) & (c_{13}+c_{44})p & (e_{31}+e_{15})p\\ (c_{13}+c_{44})p & (c_{44}+c_{33}p^2) & (e_{15}+e_{33}p^2)\\ (e_{31}+e_{15})p & (e_{15}+e_{33}p^2) & -(\varepsilon_{11}+\varepsilon_{33}p^2)\end{bmatrix}\begin{bmatrix}a_1\\ a_3\\ a_4\end{bmatrix}=\begin{bmatrix}0\\ 0\\ 0\end{bmatrix}. \tag{C7}$$

Note that the determinant is a third-order polynomial in p^2. The characteristic equation can be written

$$(p^2+\alpha^2)(p^4+2\rho\xi^2p^2+\xi^4)=0. \tag{C8}$$

The dimensionless numbers α, ρ and ξ depend on the constitutive constants; a short computer code is needed to determine them. For stable materials, they are real and restricted so that

$$\alpha>0, \quad \xi>0, \quad \rho>-1. \tag{C9}$$

The roots with positive imaginary parts are

$$p_3=i\alpha, \quad p_{1,2}=\begin{cases} i\xi(n\pm m), & \rho>1 \\ \xi(in\pm m), & \rho<1, \end{cases} \tag{C10}$$

where

$$n=\left(\frac{1+\rho}{2}\right)^{1/2}, \quad m=\left(\frac{|1-\rho|}{2}\right)^{1/2}. \tag{C11}$$

The expressions for the matrices are cumbersome in appearance, and it is probably best to proceed numerically at this point.

Due to the symmetry of the problem and its role in (5.16), the real part of Y has the structure

$$\operatorname{Re} Y=\begin{bmatrix} \dfrac{1}{C_L} & 0 & 0 \\ 0 & \dfrac{1}{C_T} & \dfrac{1}{e} \\ 0 & \dfrac{1}{e} & -\dfrac{1}{\varepsilon} \end{bmatrix}, \tag{C12}$$

where the elements should be computed numerically.